Plasma depletion layer: Event studies with a global model

Y. L. Wang, J. Raeder, and C. T. Russell
Institute of Geophysics and Planetary Physics, University of California, Los Angeles, California, USA

T. D. Phan and M. Manapat
Space Science Laboratory, University of California, Berkeley, California, USA

Received 26 January 2002; revised 18 June 2002; accepted 28 August 2002; published 10 January 2003.

[1] The plasma depletion layer (PDL) is a layer on the sunward side of the magnetopause with lower plasma density and higher magnetic field compared to the corresponding upstream magnetosheath values. In this study we use global simulations of the solar wind-magnetosphere-ionosphere system to compare with Wind PDL observations on the flanks of the magnetopause on 12 January 1996 and 1 January 1999. The consistency between model results and observations shows that the magnetohydrodynamic (MHD) description of the plasma is sufficient to describe the PDL process observed in this region. The simulation also shows that the PDL is stable as long as the interplanetary magnetic field (IMF) has no major variations. Temporal-spatial ambiguities are analyzed for the 1996 event, and a significant difference between the time series and the instantaneous PDL spatial structure is found. A much smoother instantaneous PDL spatial structure is found than observed in the simulated spacecraft time series, which is highly modulated by solar wind and IMF variations. The local time and latitude dependence of the PDL for the 1996 evento are also obtained from the model that predicts that a thinner PDL occurs near the subsolar point and a thicker PDL exists farther away from that point. *INDEX TERMS:* 2724 Magnetospheric Physics: Magnetopause, cusp, and boundary layers; 2728 Magnetospheric Physics: Magnetosheath; 2784 Magnetospheric Physics: Solar wind/magnetosphere interactions; 2740 Magnetospheric Physics: Magnetospheric configuration and dynamics; *KEYWORDS:* plasma, depletion, layer, PDL, MHD, simulation

Citation: Wang, Y. L., J. Raeder, C. T. Russell, T. D. Phan, and M. Manapat, Plasma depletion layer: Event studies with a global model, *J. Geophys. Res.*, *108*(A1), 1010, doi:10.1029/2002JA009281, 2003.

1. Introduction

[2] The study of the magnetosheath field and flow structure near the magnetopause has attracted a lot of attention because it affects the coupling of mass, momentum, and energy between the solar wind and the magnetosphere. When the IMF is southward ($B_z < 0$), magnetic reconnection takes place at the subsolar magnetopause and substantial amounts of energy, mass, and momentum can be directly transferred from the solar wind into the magnetosphere, powering magnetospheric phenomena, such as the aurora. The linkage of the magnetosphere and magnetosheath magnetic fields leads to transfer of magnetic flux into the magnetotail. The flux transfer event (FTE) [*Russell and Elphic*, 1978] is an unsteady form of this transfer. However, when the IMF is northward and the magnetic shear across the magnetopause is low, no reconnection flow signatures are observed near the subsolar magnetopause. During such periods, the interplanetary magnetic field lines tend to pile up near the magnetopause and the plasma pressure and density and/or temperature decrease to keep the total pressure in balance. The resulting layer is then called the plasma depletion layer (PDL). Its main characteristics are a lower plasma density and a higher magnetic field values compared to their corresponding upstream magnetosheath values. The conditions for the formation of the PDL can be more complex than what we have mentioned above. For example, the PDL can form for southward IMF under high solar wind dynamic pressure conditions and could be related to the limitation of reconnection flows for high solar wind Mach numbers [*Anderson et al.*, 1997].

[3] Observational evidence for a PDL just outside of the magnetopause has been reported by many authors [e.g., *Cummings and Coleman*, 1968; *Freeman et al.*, 1968; *Crooker et al.*, 1979; *Fuselier et al.*, 1991; *Song et al.*, 1993a; *Paschmann et al.*, 1993; *Anderson and Fusier*, 1993; *Anderson et al.*, 1994; *Phan et al.*, 1994, 1997]. It was first studied theoretically by *Zwan and Wolf* [1976], who proposed two processes for depleting flux tubes. First, by deflecting plasma around the magnetosphere the bow shock pushes plasma out along the field lines away from the nose of the magnetosphere. Second, they claimed that the compressional stress exerted on magnetosheath flux tubes near the nose tends to squeeze plasma out along the field lines, further depleting them. However, there are intrinsic discrepancies in Zwan and Wolf's model. Based on ISEE magnetosheath observations [*Song et al.*, 1990; *Song and Russell*,

0148-0227/03/2002JA009281$09.00

1992], *Southwood and Kivelson* [1992] considered the problem from the point of view of MHD waves and proposed a different model for the creation of the PDL. Later, *Southwood and Kivelson* [1995] attempted to reconcile the discrepancies between these two models. In their new scenario, as can be seen in Figure 3 in their paper, three regions were identified: (i) an upstream region where the flow is insufficiently deflected to move around the boundary; (ii) a frontal region where deflection of the flow is imposed; (iii) a region of depletion against the magnetopause. In these three regions, normal magnetosheath density and magnetic field, compressed density and rarefied magnetic field, and compressed magnetic field and rarefied density exist, respectively. Further theoretical studies of the PDL were presented by [*Farrugia et al.*, 1995, 1997a, 1997b], who particularly addressed the variation of the PDL structure with changing solar wind Mach number and the possible existence of the PDL in front of an interplanetary magnetic cloud. In all of these studies, ideal MHD theory is used to model the PDL.

[4] However, questions about the nature of the PDL remain. For example, whether MHD effects or kinetic effects dominate the PDL, whether anisotropy, as present in many PDL observations, is a cause or consequence of the PDL, how is the PDL affected by transient solar wind conditions, and whether the PDL exists in a stable manner or in a transient fashion. To solve these problems, numerical simulations are a natural next step. *Omidi and Winske* [1995] have compared the results of one-dimensional Hall-MHD and hybrid simulations to the observed structure of the magnetopause. They found that the fluid solutions consist of discontinuities such as slow shocks, but kinetic solutions consist of fewer discontinuities and include non-MHD boundaries. They argued that kinetic solutions are found to be in a much better agreement with magnetopause observations. *Winske and Omidi* [1995], using hybrid simulations, reached the conclusion that diffusion due to low frequency waves, such as slow waves, is not likely to be a major effect on the magnetopause during northward IMF. *Wu* [1992] simulated large-scale three-dimensional MHD flow in the idealized magnetosheath with a perfectly conducting sphere as the magnetopause. The PDL is seen as the result of increasing magnetic field near the magnetopause. However, his simulation produced much larger PDL thickness than observed, which was attributed by *Lyon* [1994] to the high numerical dissipation in Wu's code. *Lyon* [1994] used MHD simulations with much less numerical dissipation and similar boundary conditions to study the magnetosheath pattern and the PDL structure. He found that slow wave modes can only exist for low Mach number cases and no evidence of such mode waves exist for typical solar wind. This is inconsistent with some observational results [*Song et al.*, 1990; *Song and Russell*, 1992] and he was unable to determine whether the observed density enhancement is an ideal MHD phenomenon or not. Meanwhile, he argued that greater resolution is needed to study the stagnation region and the near magnetopause structure for high Mach number solar wind flow. *Denton and Lyon* [2000] studied the effects of pressure anisotropy on the magnetosheath structure using a two-dimensional MHD simulation with anisotropic pressure by assuming a flux surface magnetopause. They found that the exact form of the parallel pressure gradient force may not be crucial for global dynamics of the PDL. The anisotropy leads to a larger bow shock standoff distance compared to the isotropic case due to the difference in perpendicular pressure. Their results also imply that the effects of pressure anisotropy may be even less for a three-dimensional system than for a two-dimensional system.

[5] Because the width of the PDL is relatively small, that is, usually around 0.5 R_E or less, it can reasonably be expected that single satellite observations capture the PDL structure perpendicular to the magnetopause. However, we know very little about the global structure, because there are no multiple simultaneous observations at large separations available. The situation is further complicated by the fact that the solar wind and IMF are rarely steady. Thus it is often difficult, if not impossible, to discern spatial structure from temporal variability using single spacecraft observations near the magnetopause. This not only makes it difficult to study the PDL experimentally, but also makes it difficult to compare theoretical models with observations, because theoretical models like those presented by Zwan and Wolf or Southwood and Kivelson assume idealized steady conditions.

[6] Global numerical models, on the other hand, offer the possibility of real event studies, that is, using observed solar wind and IMF parameters to drive the model, and comparing the results of the simulation with in situ observations near the magnetopause. With this approach several issues can be attacked simultaneously. First, the quality of the match between the simulation result and the observation tells us whether or not the formalism underlying the simulation is adequate to describe the process. In this study, we use an MHD based code, thus with the event studies presented in this paper we will demonstrate that at least in two typical PDL cases the processes leading to the formation of a PDL are well within the realm of MHD and no other processes need to be invoked. Of course, resolving the remaining issues depends on favorable model-data comparison. Second, the model allows us to investigate what the spacecraft really saw. In particular, we can compare the time series taken along the spacecraft trajectory with a spatial cut along the trajectory at a given time. This allows us to resolve the spatial-temporal ambiguities that are inherent in the single spacecraft observations. Third, the simulation provides us with a global view of the PDL, both in space and time. In particular, we can investigate its spatial extent (including local time and latitude extent), how its thickness and other properties vary along the magnetopause, and how it develops in time. This includes also the response of the PDL to transient structures in the solar wind and the IMF. Fourth, the simulation provides us clues as to the particular observations needed to constrain its properties experimentally. Clearly, more observations will require multiple spacecraft, possibly many. However, the number of required spacecraft and their orbits are far from clear at present time.

[7] In this paper we address the first and the second issues. The predicted local time and latitude extent are also addressed to show the potential of the model in studying the global structure of the PDL. We present two event studies in which we compare our simulation results with in situ measurements. The excellent match between the simulation results and the observations makes us conclude that along

the flanks the PDL formation can be treated with an MHD formalism. We also address the stationarity of the PDL by comparing model time series results with corresponding cuts at certain time instants. Finally, we show the local time and latitude extent of the PDL in the first event.

2. Event Selection

[8] PDL observations are rare, particularly those with simultaneous solar wind and IMF data. There are two reasons why we need simultaneous solar wind and IMF observations: First, our global model needs those observations as input; second, and more important, magnetosheath variations are usually temporal, controlled by solar wind and IMF changes. Thus it is necessary to compare solar wind and magnetosheath observations to make sure that the structures in the magnetosheath are of internal origin and not structures convected from solar wind. We exclude PDL events with southward IMF B_z to avoid effects of subsolar reconnection on the PDL. We examine two events, based on the characteristics of clear PDL signatures, the availability of three dimensional sheath flow measurements, and solar wind and IMF data: the PDL event on 12 January 1996 that was previously published by *Phan et al.* [1997] and an event on 1 January 1999.

2.1. The 12 January 1996 Event

[9] The trajectories of the Wind and IMP 8 spacecraft during the 12 January 1996 event are shown in Figure 1. The IMP 8 spacecraft stays outside of the bow shock from 1300 to 2100 UT and provides solar wind and IMF observations for this PDL event, while Wind passes through the bow shock, the magnetosheath, and the magnetopause and provides the PDL observations. Wind and IMP 8 observations for this event are shown in Figure 2. From top to bottom in Figure 2 are plasma velocity, magnetic field clock angle in GSE yz plane, the ratio of B_x to magnetic field magnitude, magnetic field magnitude, plasma density, and plasma temperature. Note that IMP 8 magnetic field magnitudes are multiplied by a factor of 3 and density values are multiplied by a factor of 2.2 for better comparison between solar wind and magnetosheath observations. Since Wind and IMP 8 are very close to each other in the Sun-Earth direction, no time delay between them is considered when we compare their observations. More complete observations for this event are shown in Figure 2 in [*Phan et al.*, 1997]. From 1300 to 2100 UT, Wind moves inbound from (5.8, 19.6, 0.7) R_E to (−3.8, 14.6, −0.3) R_E, i.e., very close to the z = 0 plane in GSE coordinates and near the dusk flank of the magnetopause and from 74° to 109° solar zenith angle. At ∼1510 UT Wind reaches bow shock, as evident from the jump of plasma density and temperature, and the decrease of plasma velocity. A sharp increase of the plasma β values is also observed from ∼1 upstream of the shock to ∼10 downstream of the shock, which means that the plasma is dominant in controlling the motion in the magnetosheath. Behind the bow shock, Wind stays in the magnetosheath from 1510 to 2000 UT. As pointed out by *Phan et al.* [1997], a sharp increase of the plasma density values is observed in the early part of the Wind magnetosheath passage. About an hour later the density drops to relatively

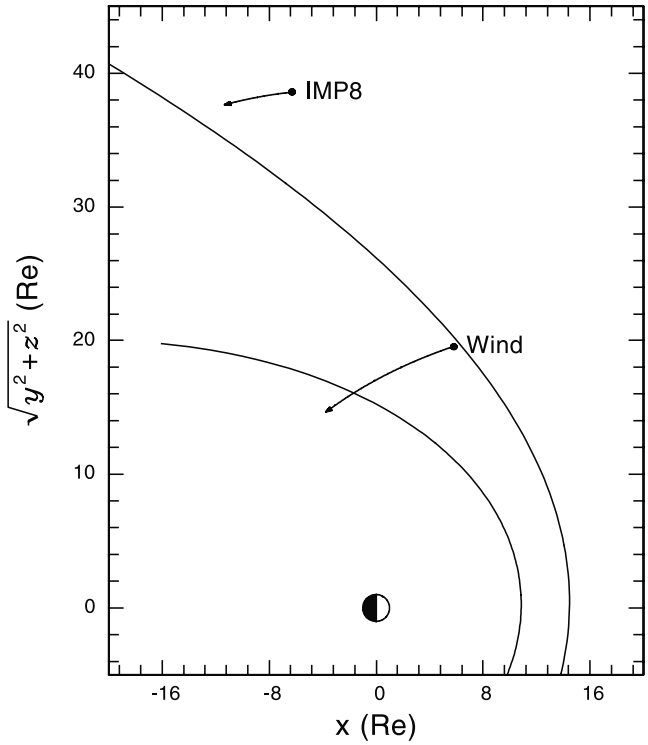

Figure 1. Wind and IMP 8 trajectories for the 12 January 1996 PDL event. IMP 8 moves from (−6.3, 31.2, 22.7) R_E to (−11.3, 30.4, 22.1) R_E from 1300 to 2100 UT, which is outside of the bow shock in the solar wind. Wind moves from (5.8, 19.6, 0.7) R_E to (−3.8, 14.6, −0.3) R_E across the bow shock, the magnetosheath, and the magnetopause. Bow shock and magnetopause curves are calculated using the empirical *Fairfield* [1971] model.

smaller values. There is no obvious solar wind density structure in the IMP 8 observations that might correspond to this magnetosheath density structure. However, the IMF does rotate at this time and, as we show later, the MHD model using IMP 8 data as input does reproduce a density enhancement at this time. The plasma velocity is less structured. It first decreases behind the bow shock and then increases as Wind approaches the magnetopause. The velocity increase before the magnetopause was interpreted as due to the $\mathbf{J} \times \mathbf{B}$ force [*Phan et al.*, 1997]. Close to the magnetopause, an obvious density decrease and a magnetic field magnitude increase occur, which is identified by *Phan et al.* [1997] as a PDL. The PDL structure is not correlated with any change in the solar wind plasma. However, there is a change in the IMF orientation coincident with the onset of the decrease in the density identified with the PDL. We do not believe the PDL is affected by this change in the IMF because the variation in the PDL is gradual while the IMF change was abrupt. After crossing the magnetopause, Wind enters the LLBL which is characterized by a very sharp decrease of plasma velocity, density, and magnetic field magnitude, together with a very sharp increase of plasma temperature.

[10] During the Wind inbound passage from 1300 to 2100 UT IMP 8 also moves inbound from (−6.3, 31.2, 22.7) R_E to (−11.3, 30.4, 22.1) R_E. It is located downstream of Wind,

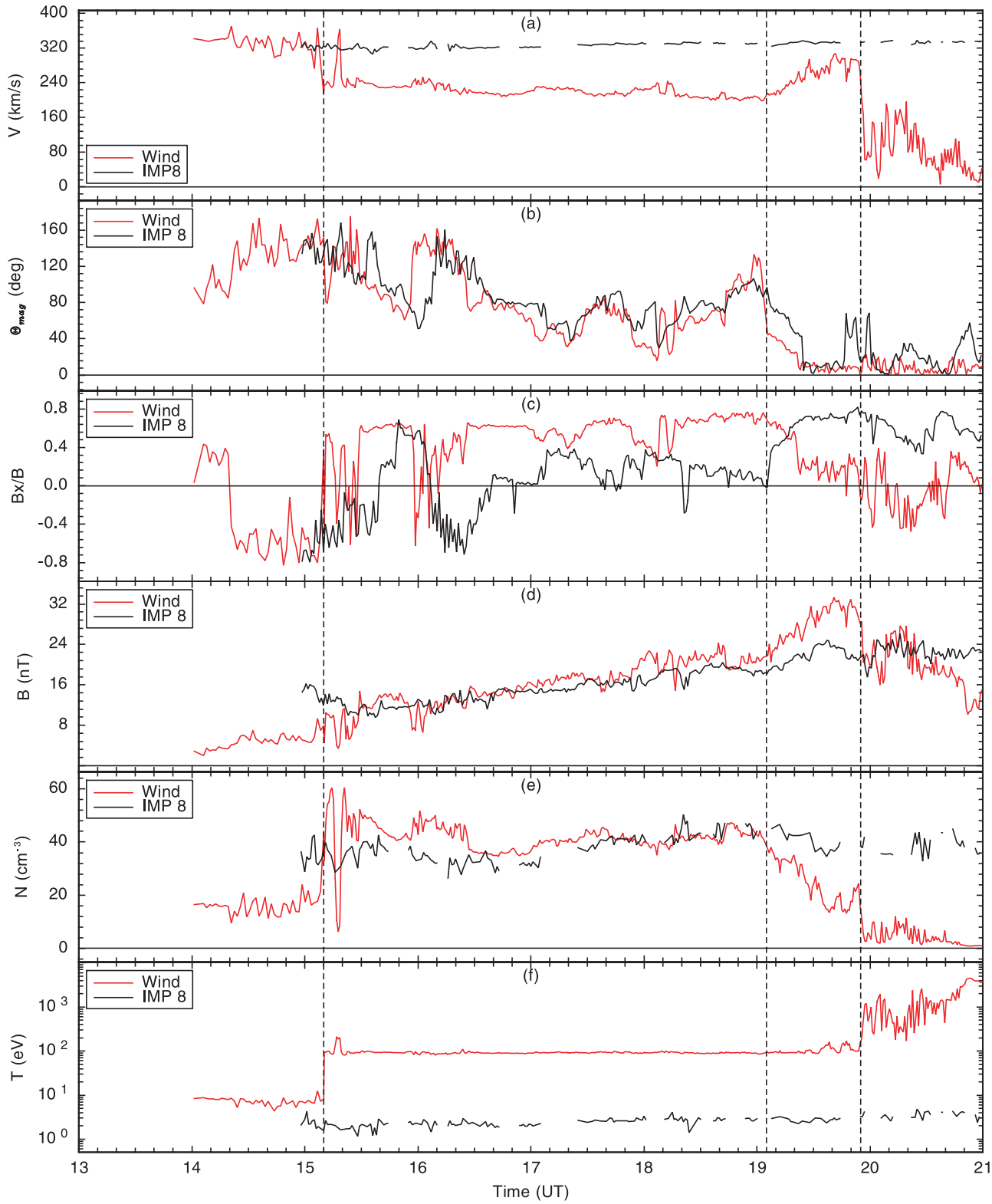

Figure 2. Wind and IMP 8 observations for the 12 January 1996 event. (a–f) Plasma velocity, magnetic field clock angle in GSE yz plane, the ratio of B_x to magnetic field magnitude, magnetic field magnitude, plasma density, and plasma temperature. Note that IMP 8 magnetic field magnitudes are multiplied by a factor of 3 and density values are multiplied by a factor of 2.2 for better comparison between solar wind and magnetosheath observations. The vertical dash lines from left to right correspond to the bow shock, PDL outer boundary, and the magnetopause, respectively.

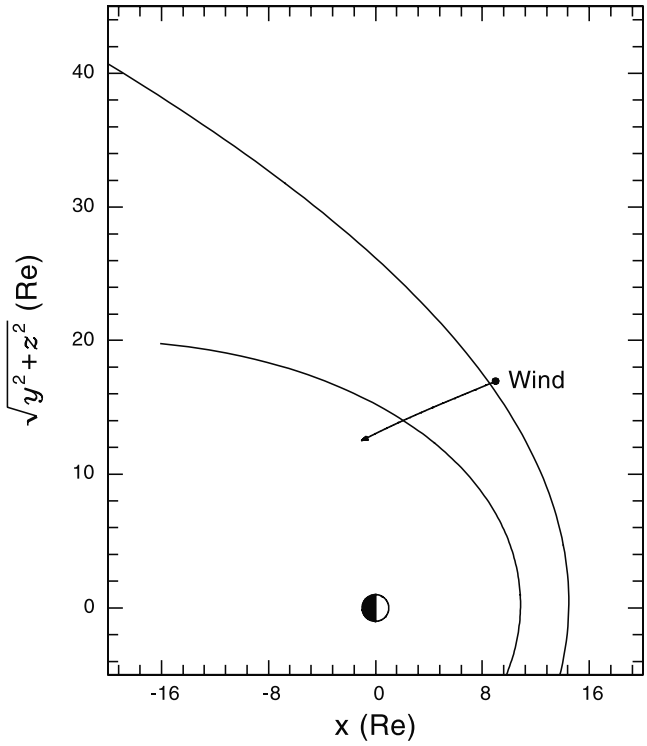

Figure 3. Wind trajectory for the 1 January 1999 PDL event from 1400 to 2400 UT. During this period, Wind moves inbound from (9.0, 9.3, −14.2) R_E to (−1.0, 11.8, −4.2) R_E through the magnetosheath and the magnetopause into the plasma sheet, while ACE stays around (226, 38, −2) R_E upstream in the solar wind. Bow shock and magnetopause curves are calculated with the empirical *Fairfield* [1971] model.

but remains upstream of the bow shock because of its large distance from the Sun-Earth line. During this period, the IMP 8 solar wind and magnetic field observations are rather stable. No obvious structures exist that would correspond to the PDL structure, though there are correlations between magnetosheath and solar wind parameters which will be discussed later. A more complete analysis of this event can be found in *Phan et al.* [1997].

2.2. The 1 January 1999 Event

[11] The Wind trajectory for the 1 January 1999 event is shown in Figure 3. The ACE spacecraft provides solar wind and IMF observations from a position near the L1 Lagrangian point. Wind and ACE observations for this event are shown together in Figure 4. From top to bottom are plasma velocity, magnetic field clock angle in GSE yz plane, the ratio of B_x to magnetic field magnitude, magnetic field magnitude, plasma density, and plasma temperature. Note that ACE magnetic field magnitudes are multiplied by a factor of 3 and density values are multiplied by a factor of 2.2 for better comparison between solar wind and magnetosheath observations. Since ACE is ~225 R_E upstream of the Earth, we need to consider a delay of ~55 min when we relate Wind observations with those of ACE. Such a time delay is included in Figure 4. From 1400 to 2400 UT, Wind moves inbound from (9.0, 9.3, −14.2) R_E to (−1.0, 11.8, −4.2) R_E and from a solar zenith angle of 62° to 95°. During this period it passes from the solar wind across the bow shock, the magnetosheath, the magnetopause, the LLBL, and eventually into the plasma sheet. At ~1550 UT Wind crosses the bow shock. Behind the bow shock, Wind stays in the magnetosheath from 1550 to 2200 UT. There is no distinct high density structure right after the bow shock as observed in the former event. The plasma velocity decreases as Wind approaches the magnetopause. Unlike in the first event, there is no accelerated plasma flow in the PDL layer. As Wind approaches the magnetopause at ~2200 UT, the plasma density decreases over a period of nearly two hours with a simultaneous increase of the magnetic field. We identify this structure as a PDL. Clearly, the magnetic field increase and the density decrease are not correlated with the solar wind, but as before the onset of the PDL occurs at an IMF discontinuity. Like in the previous case we do not believe that this IMF discontinuity affects the PDL because of its abruptness compared to the PDL structure. After crossing the magnetopause, Wind enters the LLBL. The velocity and plasma density drop to smaller values over a very short time. Unlike case 1 there is very little change of the magnetic field values across the magnetopause.

[12] During the Wind inbound passage from 1400 to 2400 UT, ACE only moves slightly and basically stays near (226, 38, −2) R_E. During this period, ACE's solar wind parameters are rather stable and the magnetic field remains northward during Wind PDL crossing. Note that in panel (b) of Figure 4 there is a prolonged southward IMF B_z period from 1930 to 2010 UT in the ACE observations. However, there is only a comparatively short period of southward B_z in the Wind observations during this time. Since the bow shock does not change the magnetic clock angle in yz plane in a significant way, we believe that the most likely explanation for this difference is that the solar wind field structure observed at ACE is different from the one that impacts the Earth because ACE is ~200 R_E upstream in the solar wind from the Earth and it is ~40 R_E away from the Sun-Earth line. Such difference can have significant effects for model results, as we will show later in this paper.

3. Model

[13] The UCLA/NOAA global geospace model is used in this study. This model solves the MHD equations in a large volume surrounding the Earth such that the entire interaction region between the solar wind and the magnetosphere is included. Specifically, the simulation domain comprises the bow shock, the magnetopause, and the magnetotail up to several hundred R_E from the Earth. It can be driven by real solar wind plasma and IMF observations. NOAA Coupled Thermosphere Ionosphere Model (CTIM) is included to handle the coupling between the magnetosphere and the ionosphere. The MHD model is discussed in more detail by *Raeder* [1999], the CTIM model is discussed in detail by *Fuller-Rowell et al.* [1996], and the coupled model was first presented in detail by *Raeder et al.* [2001a].

[14] In the 12 January 1996 event, the Wind spacecraft passes through the magnetopause at the dusk side magneto-

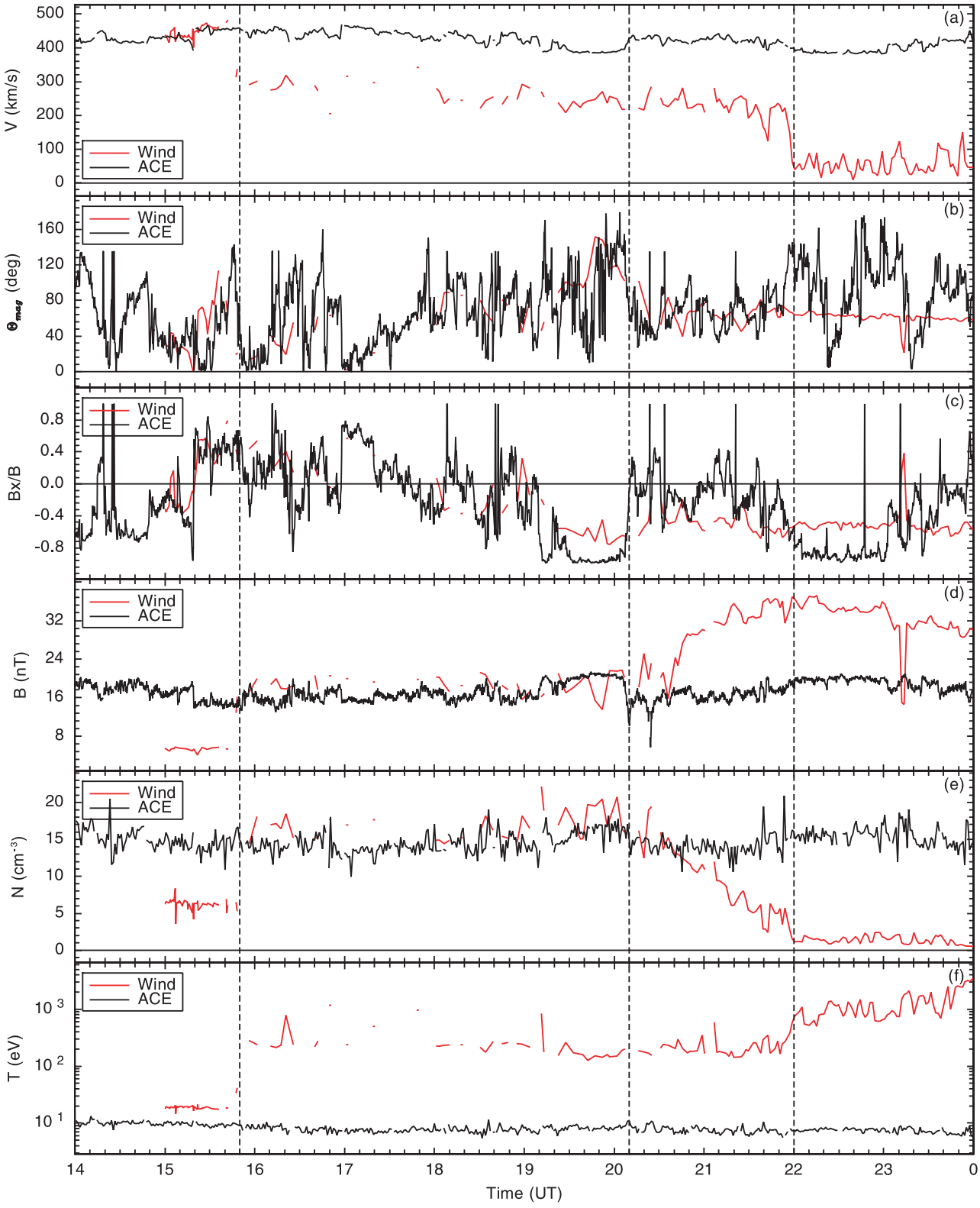

Figure 4. Wind and ACE observations for the 1 January 1999 PDL event. (a–f) Plasma velocity, magnetic field clock angle in GSE yz plane, the ratio of B_x to magnetic field magnitude, magnetic field magnitude, plasma density, and plasma temperature. Note that ACE magnetic field magnitudes are multiplied by a factor of 3 and density values are multiplied by a factor of 2.2 for better comparison between solar wind and magnetosheath observations. The vertical dash lines from left to right correspond to the bow shock, outer PDL boundary, and the magnetopause, respectively. It takes ~55 min for solar wind to convect from ACE to Wind, and the ACE data are shifted this amount of time in the figure for better comparison.

pause flank, which is about y = 15 R_E and z = 0 R_E. In the 1 January 1999 event, the Wind spacecraft passes through the magnetopause also at its dusk flank but in the southern hemisphere at about y = 15 R_E and z = −8 R_E. For the simulations presented here we have adapted the MHD grid such that the best resolution is obtained in the vicinity of the spacecraft orbit of interest. Specifically, within a few R_E of the spacecraft trajectory the grid size is ∼0.2 R_E. We will show later that this resolution is sufficient to resolve the PDL.

[15] Solar wind density, pressure, velocity, and magnetic field observed by IMP 8 and ACE are used as the input of the global model in the two simulations, respectively. The data gaps in the IMP 8 observations during the simulation period are filled by linear interpolation. Because of the difficulty of using B_x observations as model input, we set the solar wind B_x component to zero in the simulations presented here. *Raeder et al.* [2001b] have shown that the influence of IMF B_x is small for the magnetosphere processes when IMF B_x is smaller compared to the other IMF components. In next section, we show that B_x plays an insignificant role in the magnetosheath and the PDL processes even during periods when B_x is larger compared to the other IMF components. The simulation runs cover the period 1300 to 2100 UT for the first event and 1400 to 2400 UT for the second event.

4. Results

4.1. The 12 January 1996 Event

[16] The model time series results along Wind trajectory during this event are shown in Figure 5, along with the Wind data. From top to bottom in Figure 5 are plasma velocities perpendicular and parallel to the local magnetic field, magnetic field three components B_x, B_y, and B_z, magnetic field magnitude B, plasma density, plasma temperature, the ratio of plasma density to magnetic field magnitude (N/B), and field line connectivity (to be defined later). The simulation shows the bow shock crossing slightly later than observed by Wind (spatial distance is ∼0.75 R_E which is about three times the local grid size). However, the difference is insignificant for this study and it can be attributed to the limited spatial resolution of the simulation near the bow shock, the missing B_x in the model input, and the neglect of pressure anisotropy. During the remaining Wind passage in the magnetosheath the model results fit well with Wind observations. In particular, the PDL structure with lower plasma density and higher magnetic field as observed by Wind is reproduced. The velocity values perpendicular and parallel to the local magnetic field also fit well with Wind observations during this period, with only small shifting of ∼50 km/s in the perpendicular velocity values in the PDL region. During the entire Wind magnetosheath passage, including the PDL, model temperature values are highly consistent with observations. After 1955 UT, the LLBL and the plasma sheet are encountered and the model results deviate more significantly from the observations. Specifically, a sharp perpendicular velocity drop observed by Wind is not fully reproduced by the model. The model shows plasma perpendicular velocity decrease but at a much slower rate, until the velocity reaches the observed values at ∼2020 UT. The model parallel velocity values fit well with Wind observations during the transition from the PDL to the LLBL and inside the magnetopause. In contrast to the decreasing values of the total magnetic field observed by Wind, the model total magnetic field increases slowly from 1955 to 2100 UT. Density values experience the same trend as the perpendicular velocity, i.e., a smooth decrease instead of a sharp drop of the plasma density is obtained in the model. A large difference between the model and the observed temperatures occurs inside the magnetopause. This can be attributed to the fact that no high energetic ring current particles are included in the model. Model N/B values fit well with observations too, and there is a sharp transition of N/B values before and after the PDL, which is expected for the PDL. This implies that N/B can be used as an effective measure to identify the PDL structure.

[17] To complement the visual evaluation of the fit between model and observations, here we also calculate the standard deviations of observations (SD) and average departures of model results from observations (AD), which are defined as:

$$SD = \sqrt{\frac{1}{N-1}\sum_{i=1}^{N}\left(V_{obs,i} - \bar{V}_{obs}\right)^2}, \quad (1)$$

$$AD = \frac{1}{N}\sum_{i=1}^{N}\left|V_{model,i} - V_{obs,i}\right|, \quad (2)$$

where N is the total number of data points in given time interval. The results are shown in Table 1.

[18] In Table 1, we choose three time intervals for standard deviation and average departure calculations: 16:40–19:55 UT (both the magnetosheath and the PDL), 16:40–19:05 UT (the magnetosheath), and 19:05–19:55 UT (the PDL), in order to quantify the match between model and observations. We did not include the early part of the magnetosheath passage because it is not relevant for the PDL. From Table 1 we can see that model average departures are, in most cases, smaller than or comparable to the standard deviations of the observations. Also, the model average departures are always much smaller compared to their corresponding observation values as we can see from Figure 5. In rare cases, e.g., density, temperature, and N/B in the magnetosheath, model departures (4.0 cm^{-3}, 18.7 eV, and 0.4 $cm^{-3}nT^{-1}$) are larger than the standard deviations of observations. However, these departures are still much smaller than their average background values, which are ∼100 cm^{-3}, 100 eV, and 2 $cm^{-3}nT^{-1}$, respectively.

[19] Panel (j) in Figure 5 shows the connectivity of the field lines along Wind trajectory from the model results. The connectivity of a field line is defined as the connection between this field line and the Earth. There are three types of connections: both ends of a field line connect to the solar wind (marked by a value of 0 and also called solar wind field line); one end of a field line connects to the Earth and the other to the solar wind (marked by a value of 1 and also called open field line); and both ends of a field line connect to the Earth (marked by a value of 2 and also called closed field line). Panel (j) shows that the PDL lies primarily on open field lines during this event. Because the IMF is

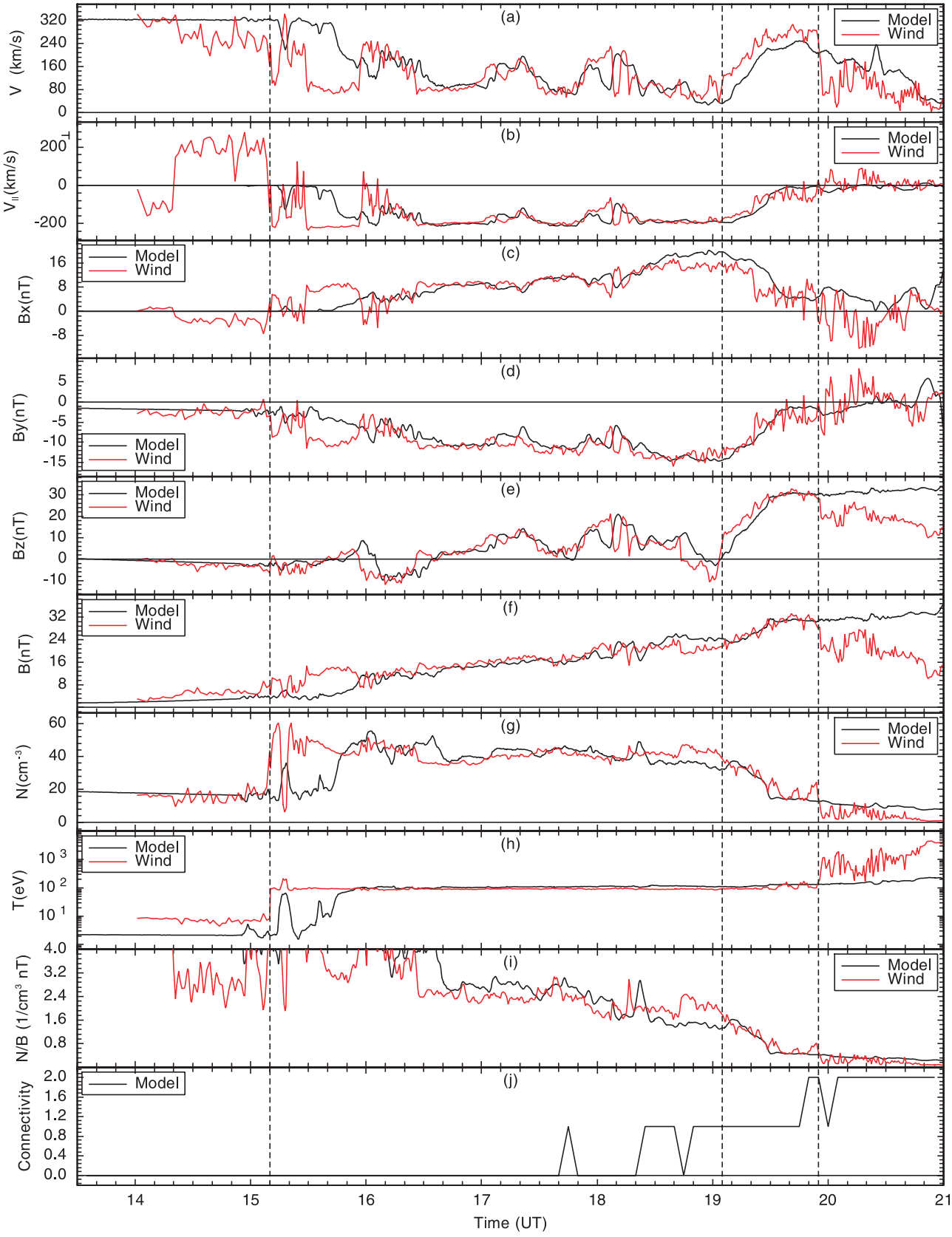

Figure 5. Comparison between the time series from the global model results along the Wind trajectory and Wind observations for the 12 January 1996 PDL event. (a–j) Plasma velocities perpendicular and parallel to the local magnetic field, magnetic field three components B_x, B_y, and B_z, magnetic field magnitude, plasma density, plasma temperature, the ratio of plasma density to magnetic field magnitude (N/B), and field line connectivity. The three vertical dash lines correspond to the three vertical lines in Figure 2.

Table 1. Standard Deviations of Observations and Average Departures of Model Results

	16:40-19:55 UT		16:40-19:05 UT		19:05-19:55 UT	
Component	SD[a]	AD[b]	SD	AD	SD	AD
$V_\perp$ (km/s)	72.6	36.2	45.6	29.7	54.1	54.6
V (km/s)	53.3	22.4	27.2	18.3	74.1	34.8
B_x (nT)	3.9	2.3	2.8	1.8	4.8	3.9
B_y (nT)	3.3	1.5	1.7	1.3	3.7	1.8
B_z (nT)	10.3	3.6	6.2	3.8	6.6	3.2
B (nT)	5.1	1.7	2.6	1.9	3.3	1.1
N (cm^{-3})	8.4	3.9	2.9	4.0	7.9	3.4
T (eV)	12.2	19.2	2.5	18.7	20.5	20.8
N/B ($1/cm^3$ nT)	0.7	0.3	0.3	0.4	0.4	0.1

[a]Standard deviation of observations.
[b]Average departure of model results from observations.

strongly northward, these field lines can experience cusp reconnection and drape over the dayside magnetopause. This might contribute to the formation of the PDL. However, more work is need to determine the detailed influence of the cusp reconnection to the PDL process, which is beyond the scope of this paper.

[20] Figure 6 shows the three-dimensional field line configuration along the Wind trajectory at 2000 UT for this event. The boundary between open and closed field lines is shown as a pink surface. The z = 0 R_E plane shows the plasma density and the y = −6 R_E plane shows the plasma pressure. Field lines along the Wind trajectory are shown with different colors: green, black, and blue, which correspond to solar wind, open, and closed field lines, respectively. The field lines that thread the PDL region are for the most part open. They obviously originate from reconnection between the IMF and the northern lobe, which is typical for northward IMF conditions. Unlike in the case of very strong northward IMF, where simultaneous reconnection of IMF field lines at the northern and the southern lobe can occur, in this case the reconnection only occurs in one hemisphere. The resulting new open field lines then drape over dayside magnetopause, as evident from Figure 6. In the magnetosheath these field lines convect tailward and will eventually become part of the lobe.

4.2. The 1 January 1999 Event

[21] The model results along the Wind trajectory during this event are shown in Figure 7, along with the Wind observations. From top to bottom in Figure 7 are plasma velocities perpendicular and parallel to the local magnetic field, magnetic field three components B_x, B_y, and B_z, magnetic field magnitude B, plasma density, plasma temperature, N/B, and field line connectivity. Similar to case 1, the location of the bow shock is not precisely determined, which is not important for our study. During the remaining Wind passage in the magnetosheath, the model results fit well with Wind observations. The PDL structure with lower plasma density and higher magnetic field as observed by Wind is also well reproduced. Model velocity values fit well with Wind plasma velocity observations during all the Wind magnetosheath passage. In particular, the model perpendicular and parallel velocity values match the Wind observed plasma velocity patterns in the PDL region. Meanwhile, the model temperature fits well with observations during the entire Wind magnetosheath passage. The model magnetic field and density values fit well with Wind observations, too. After 2200 UT, the LLBL and the plasma sheet are encountered. In contrast to the results of case 1, a sharp parallel velocity drop observed by Wind is not fully reproduced by the model. The model shows plasma parallel velocity decrease but at a much slower rate. The model perpendicular velocity values fit well with Wind observations during the transition from the PDL to the LLBL and inside the magnetopause. The different observed transition patterns for perpendicular and parallel velocities across the magnetopause in the two events are possibly related to the different latitudes for the two events. Different from case 1, the model magnetic field and density fit much better to the Wind observations inside the magnetopause. A large difference between model and observation temperature also occurs inside the magnetopause, which is similar to the first event. Model N/B values also fit well with observation N/B values inside the PDL and in most part of the magnetosheath. However, very large difference between model and observation N/B values occurs just before the PDL. The most likely cause for this large error is that, as we have mentioned in section 2.2, the IMF structure observed at ACE is not exactly the IMF structure that hits the Earth. This is a typical limitation of using solar wind and IMF observations obtained relatively far from the Sun-Earth line which requires careful consideration when comparing the model results with in situ data. We have

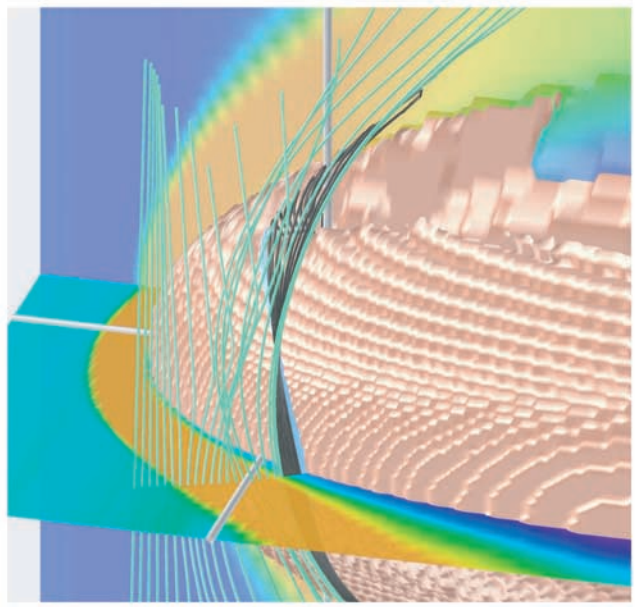

Figure 6. 3D field line configuration along the Wind trajectory at 2000 UT for the 12 January 1996 PDL event. The boundary between open and closed field lines is shown as a pink isosurface. z = 0 R_E plane shows the plasma density values and y = −6 R_E plane shows the plasma pressure values. Field lines along the Wind trajectory are shown with different colors: green, black, and blue, which correspond to solar wind, open, and closed field lines, respectively.

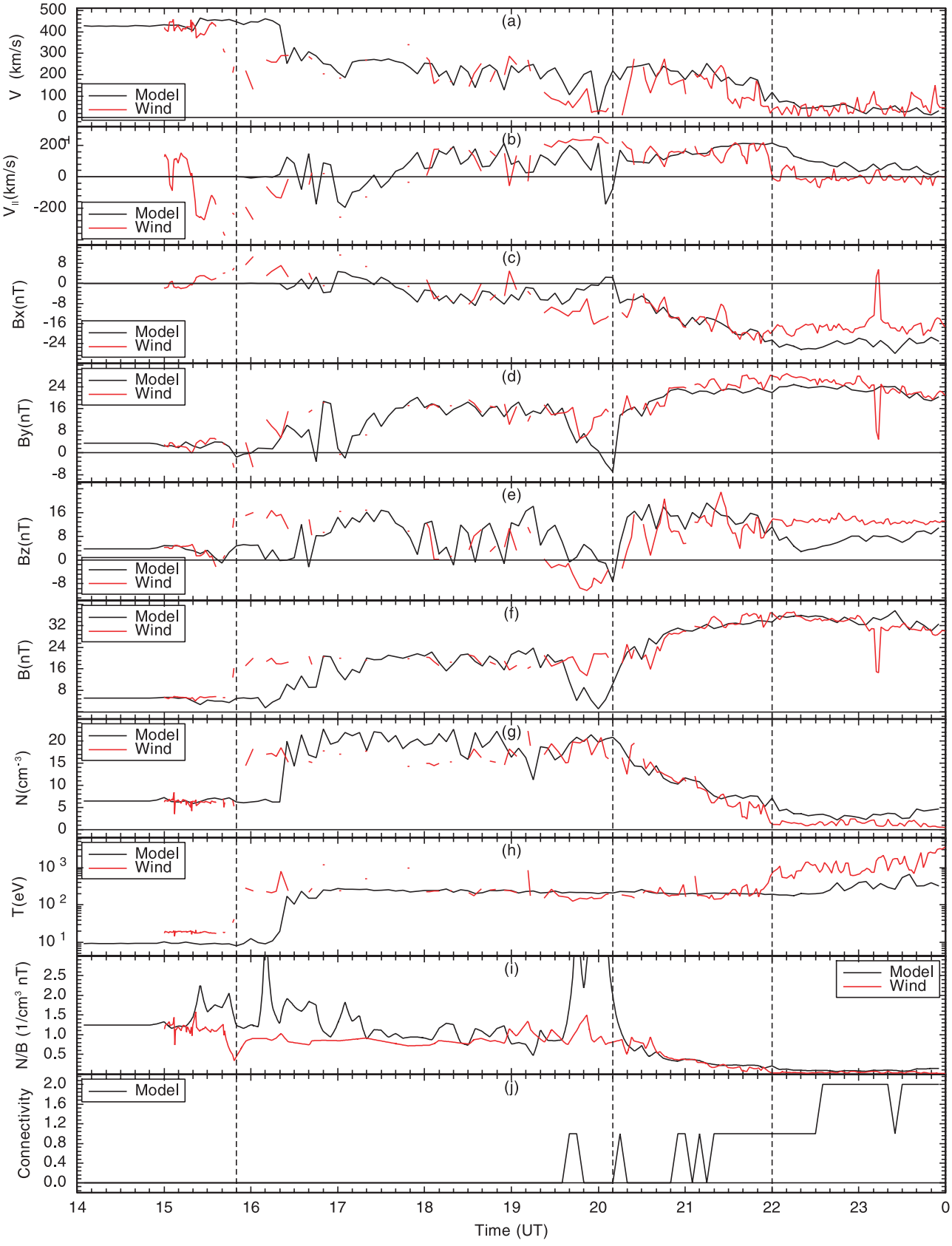

Figure 7. Comparison between the time series of the global model results along Wind trajectory and Wind observations for the 1 January 1999 PDL event. (a–j) Plasma velocities perpendicular and parallel to the local magnetic field, magnetic field three components B_x, B_y, and B_z, magnetic field magnitude B, plasma density, plasma temperature, N/B, and field line connectivity. The three vertical dash lines correspond to the three vertical lines in Figure 4.

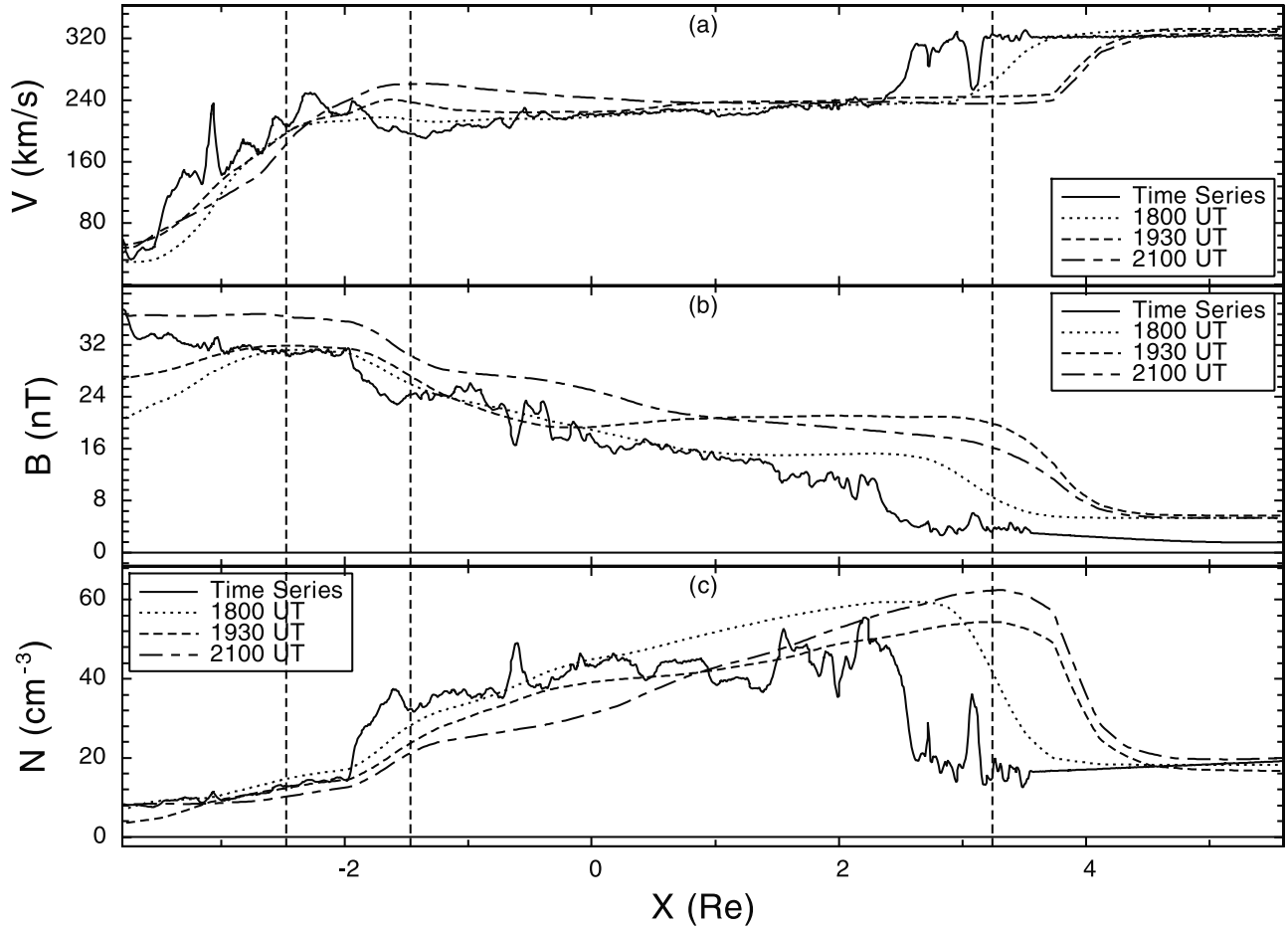

Figure 8. Snapshots along Wind trajectory from 1300 to 2100 UT for three different times: 1800, 1930, and 2100 UT for the 12 January 1996 event. Overlaid are model time series results along the Wind trajectory during this event. The panels a–c show plasma velocity, magnetic field magnitude, and plasma density. The three vertical dashed lines correspond to the three vertical lines in Figure 2 counting in opposite direction.

done the same error analysis as we did for the first event and similar results are obtained, which are not shown here.

[22] Panel (j) in Figure 7 shows the connectivity of the field lines along Wind trajectory from the model results. Similar to case 1, in the PDL region field lines are open. However, inside the magnetopause in the LLBL region, the field lines are at least partially open too, which is different from case 1.

4.3. Spatial-Temporal Ambiguities

[23] In order to have a better understanding of the PDL structure, we consider the differences between the real PDL structures and the spacecraft PDL observations. The latter are affected by both time and spatial evolutions of the PDL. Figure 8 shows plasma velocity, magnetic field magnitude, and plasma density along Wind trajectory from 1300 to 2100 UT for the 12 January 1996 event. Instead of using time series as we have done in Figure 5, here we only take snapshots of these interesting parameters along Wind trajectory during the same period for three specific times: 1930, 1800, and 2100 UT. These three times are the center of the PDL observation time at Wind, one hour and a half before and after that time. Overlapped in these panels are model time series results along Wind trajectory. Both time and spatial variations are kept in the time series results compared to the snapshot results. We plot the results versus position along the GSE x axis. One very prominent feature of the figure is that, different from the model time series results along the Wind trajectory, which fit well with Wind observations and match many fine structures in the magnetosheath and the PDL, the snapshot profiles of the model results along Wind trajectory look much smoother. The same is true for the second event. Thus, the relatively fast variations in the time series do not necessarily correspond to spatial gradients in the magnetosheath, but many of them are apparently caused by the convection of the plasma and field structures past the spacecraft. This also suggests that at any instant the real PDL structure is smoother and less structured than observed by Wind, which in fact measures convected structures as well as the spatial gradients in the magnetosheath. In Figure 8, the spatial PDL structure is similar for all the three times. This means that the PDL structure under northward IMF in the dusk flank of the magnetopause is fairly stable with time, instead of being a transient structure. Similar results are obtained for case 2. In contrast to the monotonically decreasing plasma velocity

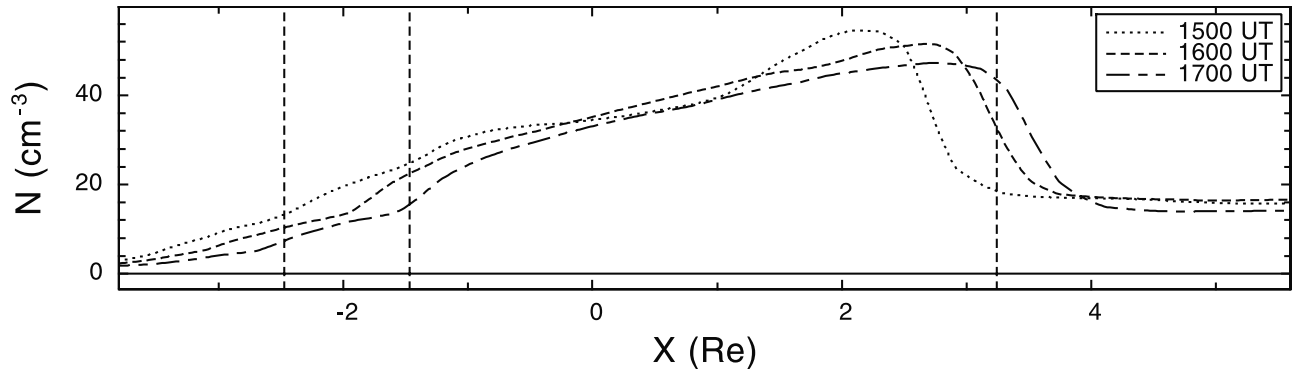

Figure 9. Density snapshots along Wind trajectory from 1300 to 2100 UT for three different times: 1500, 1600, and 1700 UT for the 12 January 1996 event. The three vertical dash lines correspond to the three vertical lines in Figure 2 counting in opposite direction.

observed by Wind in the magnetosheath before the PDL, panel (a) in Figure 8 shows that both increase and decrease of plasma velocity may exist at different times. At all three times, a velocity increase occurs at the beginning of the PDL and a velocity decrease follows in the later part of the PDL.

[24] For the distinct density peak during the early phase of the Wind magnetosheath passage in the 12 January 1996 event, in addition to the model results shown in Figure 5 , we obtain the snapshots of the plasma density along Wind trajectory from 1300 to 2100 UT for three different times: 1500, 1600, and 1700 UT as shown in Figure 9. These times are around the time when Wind observes the magnetosheath density peak structure. From the comparison it is clear that the unusual density increase at 1500 UT is just a transient feature, apparently caused by the rotation of the IMF, instead of being a stable structure downstream of the bow shock. In panel (c) of Figure 8 there is no such distinct density structure either. From IMP 8 observations we can see that this structure is likely caused by the rotation of the IMF from 1500 to 1600 UT, when Wind is passing through this density peak region (Figure 2). This is consistent with the three-dimensional MHD magnetosheath simulation results by [*Cable and Lin*, 1998] which show that high plasma density in the magnetosheath can result from the interaction between magnetic field rotational discontinuity and the bow shock. However, the density peak observed in the magnetosheath can also be the effect of foreshock cavities caused by IMF variations. *Sibeck et al.* [2000] found that the arrival of a density/pressure cavity increase bounding a cavity should cause spacecraft located in the magnetosheath just outside of the magnetopause to observe density increases. Observations and model results for the second event do not show such a density peak, however, which further confirms that such a density structure just downstream of the bow shock is not a stable structure of the magnetosheath.

4.4. Local Time and Latitude Extent of the PDL

[25] The results presented in the previous sections show that the PDL is a fairly large structure with a thickness of about 1.5 R_E at the location of the observations. However, the observations were taken far away from the subsolar region, i.e., at ~1840 LT for the 12 January 1996 event, and at ~1740 LT for the 1 January 1999 event. In order to put these results into the context of other observations which may be taken at other local times, and which usually show a much narrower PDL closer to local noon, we here investigate how the PDL thickness varies as a function of local time and latitude. Since the two previously presented events were rather similar we restrict the investigation to the 12 January 1996 event.

[26] Figure 10 shows the plasma density and magnetic field on z = 0 plane at 1900 UT for the 12 January 1996 event. Note here that the magnetic field values are clipped at 100 nT in order to make the field structures in the magnetosheath better visible. The open-closed magnetic field boundary is shown as a red zigzag curve in each of the panels. Although the model open-closed magnetic field boundary does not necessarily coincide with the magnetopause as defined by other parameters, such as temperature or current density, it is much easier to identify in the simulation results which do not provide steep gradients across the magnetopause. Also, the open-closed boundary should be fairly close to the dayside magnetopause, especially near the subsolar point. The Wind trajectory from 1300 to 2000 UT is shown as a red smooth curve in each of the equatorial cuts. On the open-closed magnetic field boundary from noon to dusk we draw a straight line for every hour local time perpendicular to the boundary pointing away from the magnetosphere. The plasma density and magnetic field magnitude along the solid straight lines in Figure 10 are shown in Figure 11. Figure 11 shows that the PDL, with the characteristics of plasma density decrease and magnetic field magnitude increase, reaches as far as 1800 LT. At the subsolar point, a sharp PDL structure with distinct density decrease and magnetic field magnitude increase can be seen. The thickness of the PDL at the subsolar point reaches ~0.3 R_E. Moving away from the subsolar point, the PDL structure becomes smoother, and the PDL becomes thicker. At 1800 LT, the PDL is still clearly discernible with a thickness of ~1.5 R_E, but the gradients of the plasma density and magnetic field magnitude in the PDL are smaller. In addition, the PDL thickness changes non-uniformly with LT. For example, the PDL thickness at 1300 LT is virtually the same as that at noon.

[27] Figure 12 shows the plasma density and magnetic field magnitude on y = 0 plane at 1900 UT for the 12

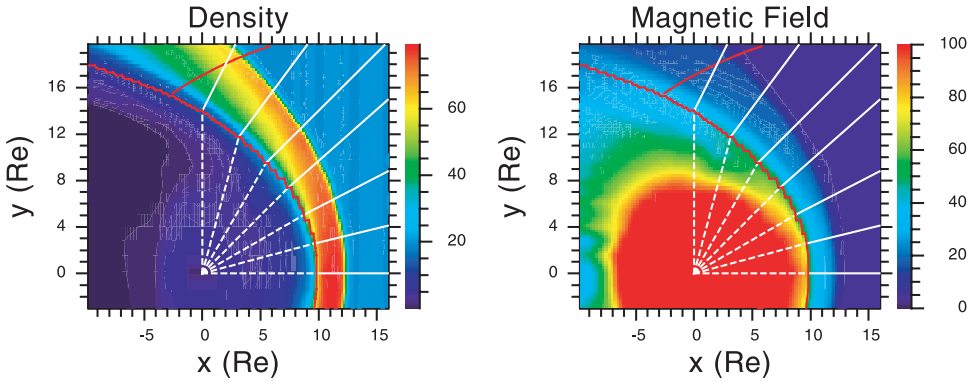

Figure 10. Plasma density and magnetic field magnitude in the z = 0 plane at 1900 UT for the 12 January 1996 event. The open-closed magnetic field boundary is shown as a red zigzag curve in each of the panels. The Wind trajectory from 1300 to 2000 UT is also shown as a red smooth curve on the top of each panel. On the open-closed magnetic field boundary from noon to dusk we draw a straight line for every hour local time perpendicular to the boundary pointing away from the magnetosphere. The plasma density and magnetic field magnitude along these solid straight lines are shown in Figure 11.

January 1996 event, in the same format as Figure 10. On the open-close field line boundary from equatorial plane poleward we draw a straight line, for every 10° until 40° latitude, perpendicular to the boundary pointing away from the magnetosphere. The plasma density and magnetic field magnitude along these solid straight lines are shown in Figure 13. Figure 13 shows that the extent of the PDL reaches as high as 40° latitude. Still, at the equatorial plane the PDL structure is the sharpest and thinnest. Moving in the poleward direction, the PDL structure becomes smoother and thicker. The PDL structure is still distinct at 40°. However, at higher latitudes, it becomes more difficult to define the PDL because of the vicinity of the cusp.

[28] In summary, the simulation shows that the PDL is thinnest at the subsolar point with a thickness of ~0.3 R_E, and the thickness increases non-uniformly both in local time and in latitude. We note, however, that the subsolar thickness is only marginally resolved by the MHD code. Thus, in reality the PDL may even be thinner near noon. We will address the PDL thickness near noon in a forthcoming investigation with better resolved simulation runs.

5. Discussion

[29] The much smoother model results for the magnetopause crossing are likely from the insufficient resolution of the model near the boundary between the magnetosheath and the LLBL. Although the model resolution is as small as 0.18 R_E near the PDL region, this grid size is still fairly coarse compared to the much smaller transition length of ~0.01 R_E quoted by *Song et al.* [1993]. As pointed out by *Winske and Omidi* [1995], diffusion does not play a significant role in the magnetopause process. However, insufficient model resolution in the transition layer, and thus higher numerical diffusion, makes the model results deviate from reality. This conclusion is consistent with the result of *Lyon* [1994], who emphasized the need of higher resolution in the PDL. Such a small grid size is very hard to achieve by a global model without more sophisticated numerical techniques like adaptive mesh refinement.

[30] In our model simulation ideal MHD with isotropic pressure is used. The good consistency of the magnetosheath structures between our model results and in situ observations indicates that pressure anisotropy is, at least for the two events that we have studied, not very important. For the 12 January 1996 event, small pressure anisotropy is observed in the magnetosheath ($T_{para}/T_{perp} \approx 0.8$) and immediately inside the magnetopause ($T_{para}/T_{perp} \approx 0.9$). The small anisotropy is consistent with the good reproduction of the observed magnetosheath features by the ideal MHD model with no anisotropy terms. Also, considering

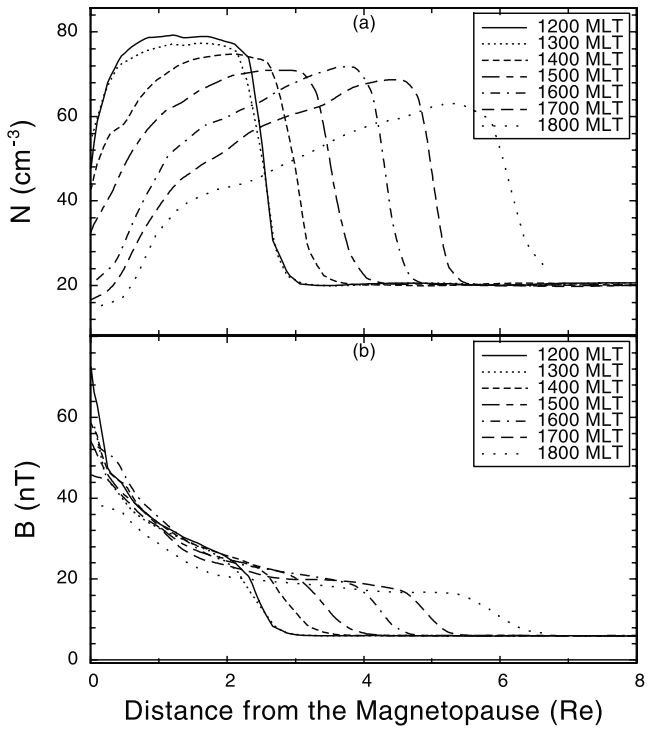

Figure 11. Plasma density and magnetic field magnitude along the solid straight lines shown in Figure 10.

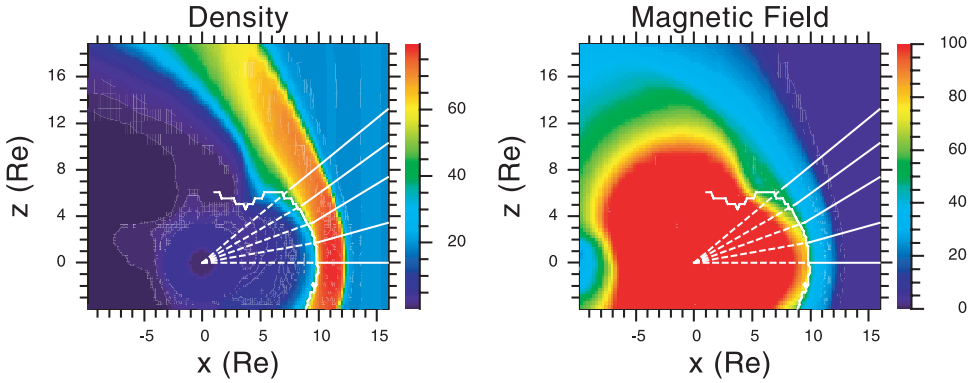

Figure 12. Plasma density and magnetic field magnitude in the y = 0 plane at 1900 UT for the 12 January 1996 event. The open-closed magnetic field boundary is shown as a white zigzag curve in each of the panels. On this boundary from equatorial plane poleward we draw a straight line every 10° until 40° latitude perpendicular to the open-close magnetic field boundary pointing away from the magnetosphere. The plasma and field properties along these solid straight lines are shown in Figure 13.

the results of *Denton and Lyon* [2000] which show that the exact form of the parallel pressure gradient force may not be critical to the global dynamics of the PDL and anisotropy effects in three-dimensional case may be less than that in two dimensional case, we can say that our isotropic MHD global model should give fairly good description of the PDL process, even when anisotropy is not very small. Because our model results deviate some what from observations in the LLBL region with even lower anisotropy in both events, it is not likely that pressure anisotropy, not included in our model, plays an important role for this inconsistency. The severe deviation between model and observation temperature inside the magnetopause implies that other mechanisms, e.g., ring current, should be included in the global model to better describe the magnetosphere region beside the PDL.

6. Summary and Conclusions

[31] The primary purpose of this paper is to test the validity of the MHD framework to study the PDL. We concentrated on two PDL events for which sufficient data are available for a meaningful comparison with the simulation results. Our findings are as follows:

1. For the two events that we studied the MHD description with isotropic pressure is sufficient to describe the PDL formation. The visual consistency between the observations and the model results is good. The average model departure is usually smaller than the standard deviation of observations and it is also usually much smaller than the corresponding normal observation values. Any other processes than isotropic MHD are thus unlikely to play an important role.

2. The PDL is stable during stable northward IMF conditions.

3. Single spacecraft observations of the PDL can be significantly different from the real spatial PDL structure. This is primarily due to the changing solar wind condition and the motion of the spacecraft relative to the magnetopause that is caused by small fluctuations of the solar wind dynamic pressure. As a consequence the observations make the PDL appear to be a lot more structured than it really is.

4. Field lines in the PDL may be either solar wind field lines or may thread the magnetopause depending on the geometry of magnetopause reconnection.

5. The PDL structure extends at least 6 hours magnetic local time away from the subsolar point on the magnetopause in the equatorial plane. Also, the PDL extends at least to 40° latitude from the equatorial plane and makes a smooth transition into the cusp. The sharpest PDL structure exists near the subsolar point and the PDL becomes smoother and thicker moving away from it.

[32] This work lays the ground for future investigations of the more general properties of the PDL. In forthcoming

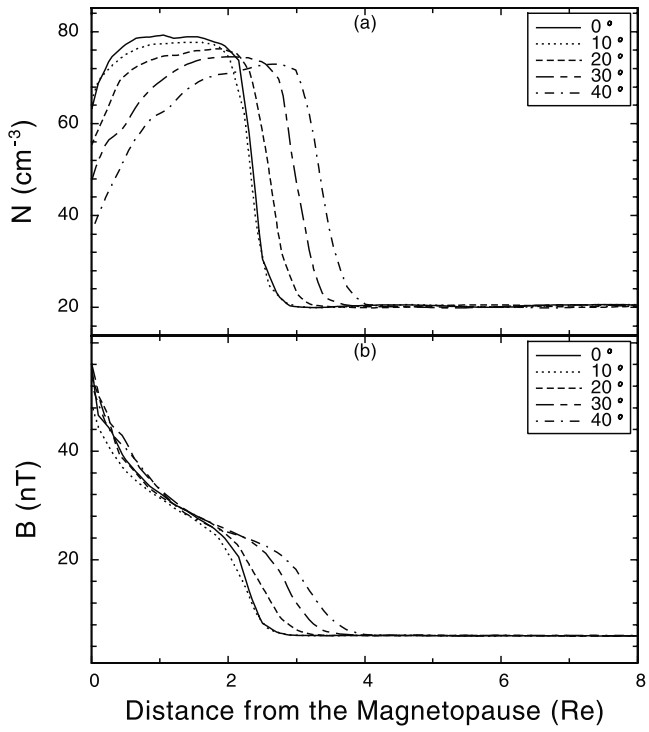

Figure 13. (a, b) Plasma density and magnetic field magnitude along the solid straight lines shown in Figure 12.

papers we will investigate the dependence of the PDL properties on solar wind and IMF conditions, as well as the effect of solar wind transients on the PDL and possibly related slow mode structures.

[33] **Acknowledgments.** The authors of the paper would like to thank C.J. Farrugia, M.G. Kivelson, P. Song, and D.J. Southwood for their very helpful discussions. We also thank the ACE SWE team, the ACE MFI team, the IMP 8 PLA team, the IMP 8 MAG team, the Wind 3DP team, and the Wind MFI team for providing the data used in this study. This work was supported by grant ATM-00-84483 and grant ATM-01-01145 from the National Science Foundation and grant NAG 5-10986 from the National Aeronautics and Space Administration. Computations were performed at the San Diego Supercomputer Center. IGPP publication number 5703.

[34] Lou-Chuang Lee and Chin S. Lin thank Richard E. Denton and Brian J. Anderson for their assistance in evaluating this paper.

References

Anderson, B. J., and S. A. Fuselier, Magnetic pulsations from 0.1 to 4.0 Hz and associated plasma properties in the Earth's subsolar magnetosheath and plasma depletion layer, *J. Geophys. Res.*, *98*, 1461, 1993.

Anderson, B. J., S. A. Fuselier, S. P. Gary, and R. E. Denton, Magnetic spectral signatures in the Earth's magnetosheath and plasma depletion layer, *J. Geophys. Res.*, *99*, 5877, 1994.

Anderson, B. J., T. D. Phan, and S. A. Fuselier, Relationships between plasma depletion and subsolar reconnection, *J. Geophys. Res.*, *102*, 9531, 1997.

Cable, S., and Y. Lin, Three dimensional MHD simulations of interplanetary rotational discontinuities impacting the Earth's bow shock and magnetosheath, *J. Geophys. Res.*, *103*, 29,551, 1998.

Crooker, N. U., T. E. Eastman, and G. S. Stiles, Observations of plasma depletion in the magnetosheath at the dayside magnetopause, *J. Geophys. Res.*, *84*, 869, 1979.

Cummings, W. D., and P. J. Coleman, Magnetic fields in the magnetopause and vicinity at synchronous orbit, *J. Geophys. Res.*, *73*, 5699, 1968.

Denton, R. E., and J. G. Lyon, Effect of pressure anisotropy on the structure of a two-dimensional magnetosheath, *J. Geophys. Res.*, *105*, 7545, 2000.

Fairfield, D. H., Average and unusual locations of the Earth's magnetopause and bow shock, *J. Geophys. Res.*, *76*, 6700, 1971.

Farrugia, C. J., N. V. Erkaev, H. K. Biernat, and L. F. Burlaga, Anomalous magnetosheath properties during Earth passage of an interplanetary magnetic cloud, *J. Geophys. Res.*, *100*, 19,245, 1995.

Farrugia, C. J., N. V. Erkaev, H. K. Biernat, and L. F. Burlaga, Dependence of magnetosheath properties on solar wind Alfvén Mach number and magnetic shear across the magnetopause, in *Proceedings of the International Workshop: The Solar Wind-Magnetosphere System 2*, edited by H. K. Biernat et al., p. 95, Austrian Acad. of Sci. Press, Vienna, 1997a.

Farrugia, C. J., N. V. Erkaev, H. K. Biernat, G. R. Lawrence, and R. C. Elphic, Plasma depletion layer model for low Alfvén Mach number: Comparison with ISEE observations, *J. Geophys. Res.*, *102*, 11,315, 1997b.

Freeman, J. W., C. S. Warren Jr., and J. J. Maguire, Plasma flow directions at the magnetopause on January 13 and 14, *J. Geophys. Res.*, *73*, 5719, 1968.

Fuller-Rowell, T. J., D. Rees, S. Quegan, R. J. Moffett, M. V. Codrescu, and G. H. Millward, A coupled thermosphere-ionosphere model (CTIM), in *STEP Report*, edited by R. Schunk, p. 217, Sci. Comm. on Sol. Terr. Phys. (SCOSTEP), NOAA/NGDC, Boulder, Colo., 1996.

Fuselier, S. A., D. M. Klumpar, E. G. Shelley, B. J. Anderson, and A. J. Coates, He^{2+} and H^{+} dynamics in the subsolar magnetosheath and plasma depletion layer, *J. Geophys. Res.*, *96*, 21,095, 1991.

Lyon, J. G., MHD simulations of the magnetosheath, *Adv. Space Res.*, *14*, 21, 1994.

Omidi, N., and D. Winske, Structure of the magnetopause inferred from one-dimensional hybrid simulations, *J. Geophys. Res.*, *100*, 11,935, 1995.

Paschmann, G., W. Baumjohann, N. Sckopke, T. D. Phan, and H. Lühr, Structure of the dayside magnetopause for low magnetic shear, *J. Geophys. Res.*, *98*, 13,409, 1993.

Phan, T. D., G. Paschmann, W. Baumjohann, N. Sckopke, and H. Lühr, The magnetosheath region adjacent to the dayside magnetopause: AMPTE/IRM observations, *J. Geophys. Res.*, *99*, 121, 1994.

Phan, T. D., et al., Low-latitude dusk flank magnetosheath, magnetopause, and boundary layer for low magnetic shear: Wind observations, *J. Geophys. Res.*, *102*, 19,883, 1997.

Raeder, J., Modelling the magnetosphere for northward interplanetary magnetic field: Effects of electrical resistivity, *J. Geophys. Res.*, *104*, 17,357, 1999.

Raeder, J., Y. L. Wang, and T. J. Fuller-Rowell, Geomagnetic storm simulation with a coupled magnetosphere-ionosphere-thermosphere model, in *Space Weather, Geophys. Monogr. Ser.*, vol. 125, edited by P. Song, H. Singer, and G. Siscoe, AGU, Washington, D.C., 2001a.

Raeder, J., et al., Global simulation of the Geospace Environment Modeling substorm challenge event, *J. Geophys. Res.*, *106*, 381, 2001b.

Russell, C. T., and R. C. Elphic, Initial ISEE magnetometer results: Magnetopause observations, *Space Sci. Rev.*, *22*, 681, 1978.

Sibeck, D. G., et al., Magnetopause motion driven by interplanetary magnetic field variations, *J. Geophys. Res.*, *105*, 25,155, 2000.

Song, P., and C. T. Russell, Model of the formation of the low-latitude boundary layer for strongly northward interplanetary magnetic field, *J. Geophys. Res.*, *97*, 1411, 1992.

Song, P., C. T. Russell, J. T. Gosling, M. Thomsen, and R. C. Elphic, Observations of the density profile in the magnetosheath near the stagnation streamline, *Geophys. Res. Lett.*, *17*, 2035, 1990.

Song, P., et al., Structure and properties of the subsolar magnetopause for northward interplanetary magnetic field: Multiple-instrument particle observations, *J. Geophys. Res.*, *98*, 11,319, 1993.

Southwood, D. J., and M. G. Kivelson, On the form of the flow in the magnetosheath, *J. Geophys. Res.*, *97*, 2873, 1992.

Southwood, D. J., and M. G. Kivelson, Magnetosheath flow near the subsolar magnetopause: Zwan-Wolf and Southwood-Kivelson theories reconciled, *Geophys. Res. Lett.*, *22*, 3275, 1995.

Winske, D., and N. Omidi, Diffusion at the magnetopause: Hybrid simulations, *J. Geophys. Res.*, *100*, 11,923, 1995.

Wu, C. C., MHD flow past an obstacle: Large-scale flow in the magnetosheath, *Geophys. Res. Lett.*, *19*, 87, 1992.

Zwan, B. J., and R. A. Wolf, Depletion of solar wind plasma near a planetary boundary, *J. Geophys. Res.*, *81*, 1636, 1976.

M. Manapat and T. D. Phan, University of California, Berkeley, Space Science Laboratory #7450, Centennial Drive at Grizzly Peak Blvd, Berkeley, CA 94720-7450, USA. (mmanapat@ssl.berkeley.edu; phan@ssl.berkeley.edu)

J. Raeder, C. T. Russell, and Y. L. Wang, IGPP/UCLA, 405 Hilgard Avenue, Los Angeles, CA 90095-1567, USA. (jraeder@igpp.ucla.edu; ctrussel@igpp.ucla.edu; ylwang@igpp.ucla.edu)